PHYSOR 2020: Transition to a Scalable Nuclear Future
Cambridge, United Kingdom, March 29th-April 2nd, 2020

Generation of the TSL for Zirconium Hydrides from Ab Initio Methods

Jonathan L. Wormald[1], Michael L. Zerkle[2], and Jesse C. Holmes[2]
[1]Naval Nuclear Laboratory
PO Box 1072, Schenectady, NY 12301-1072, USA

[2]Naval Nuclear Laboratory
PO Box 79, West Mifflin, PA 15122-0079, USA

Jonathan.Wormald@unnpp.gov, Michael.Zerkle@unnpp.gov, Jesse.Holmes@unnpp.gov

ABSTRACT

Zirconium hydride (ZrH_x) is a moderator material used in TRIGA and other reactors as well as a corrosion product in Zircaloy. ZrH_x may exist in multiple phases with varying stoichiometry, the most significant of which are the δ phase and the ϵ phase. At room temperature the δ phase is dominant for $1.56 < x < 1.64$ and the ϵ phase for $x > 1.74$. Current ENDF/B-VIII.0 ZrH_x thermal scattering law (TSL) evaluations do not distinguish between phases. These sub-libraries were generated with the LEAPR module of NJOY using historic phonon spectra derived from a central force model, and assume incoherent elastic scattering for both bound hydrogen and zirconium. While the use of incoherent elastic scattering is appropriate for hydrogen, it neglects the effects of crystal structure important for scattering from zirconium bound in ZrH_x. In this work the TSLs for hydrogen and zirconium bound in δ-ZrH_x (H-ZrH_x and Zr-ZrH_x) and ϵ-ZrH_2 (H-ZrH_2 and Zr-ZrH_2) were generated from phonon spectra derived from modern *ab initio* lattice dynamics methods and *ab initio* molecular dynamics. Density functional theory calculations were performed using the VASP code for supercells of cubic ZrH_x and of tetragonal ZrH_2 to generate partial phonon spectra for hydrogen and zirconium for each phase with the PHONON code and velocity autocorrelation function. TSLs for hydrogen and zirconium in ZrH_x and ZrH_2 were generated from these spectra using the FLASSH (Full Law Analysis Scattering System Hub) code. The generalized coherent elastic routine in FLASSH was used to generate the elastic contribution to Zr(ZrH_x) and Zr(ZrH_2), thereby capturing the previously neglected effects of crystal structure. The present TSLs provide both a re-evaluation of the current ZrH sub-libraries, and expansion of the set of TSLs available for the examination of neutrons in systems with zirconium hydride, permitting explicit treatment of δ and ϵ phases.

KEYWORDS: TSL, thermal neutron scattering, zirconium hydride

1. INTRODUCTION

Zirconium hydride is used as a moderator material in TRIGA reactors and has been historically used as a moderator in other reactors requiring high proton density for moderation (e.g., SNAP-10A [1]). Additionally, ZrH_x is a corrosion product in Zircaloy. ZrH_x exists in multiple phases

or polymorphs with varying stoichiometry [2]. The most significant of these phases are δ phase and ϵ phase, the former of which is the primary constituent of TRIGA fuel and Zircaloy corrosion [3,4]. At room temperature δ phase is dominant for $1.56 < x < 1.64$ and exists in a eutectoid mixture with α-Zirconium for $x < 1.56$. The ϵ phase is dominant for $x > 1.74$ and is mixed with δ phase for $1.64 < x < 1.74$. This stability range is approximate up to nearly 800 K. As a result of crystal binding of hydrogen in ZrH_x, energy exchange of thermal neutron scattering involves, narrow, well separated energy levels, which is in contrast to the large continuum spectra observed in other materials [5,6]. This behavior is characteristic of metal-hydrides [5,6] and greatly influences neutron thermalization effects, such as the warm neutron principle responsible for the large negative moderator feedback coefficient in TRIGA reactors.

In neutron transport calculations (e.g., Monte Carlo) of reactors, ENDF thermal scattering law (TSL) sub-libraries are used to capture the effects of crystal binding effects on low energy neutron scattering. The TSL, $S(\alpha, \beta)$, is a temperature dependent probability distribution defining the possible scattered states for an incident neutron, and has contributions from distinct effects (d) due scattered wave interference between different nuclear scattering sites and self (s) non-interference effects [7],

$$S(\alpha, \beta) = S_d(\alpha, \beta) + S_s(\alpha, \beta). \tag{1}$$

The momentum and energy transfer resulting from scattering are described by the unitless parameters α and β as,

$$\alpha = \frac{E + E' - \mu\sqrt{EE'}}{Ak_BT} \tag{2}$$

$$\beta = \frac{E' - E}{k_BT} \tag{3}$$

with μ and A representing the scattering cosine and isotope to neutron mass ratio, respectively. The incident and scattered neutron energies are E and E', and k_B and T are the Boltzmann constant and temperature. In crystals, the phonon expansion is used to compute the TSL such that [7,8],

$$S(\alpha, \beta) = \sum_p S^p(\alpha, \beta) \tag{4}$$

which is a summation of increasing orders of the convolution of the vibrational (phonon) spectra, with $p = 0$ representing elastic scattering and $p > 0$ representing inelastic scattering. In current ENDF thermal scattering sub-libraries the incoherent approximation is applied, such that distinct effects on inelastic scattering are neglected. Within this approximation the double differential scattering cross section is related to the TSL using Fermi's Golden rule as [7],

$$\frac{\partial^2\sigma}{\partial\Omega\partial E'} = \frac{1}{k_B T}\sqrt{\frac{E'}{E}}\left(\sigma_{coh}\left(S_d^0(\alpha,\beta) + S_s^0(\alpha,\beta) + \sum_{p>0} S_s^p(\alpha,\beta)\right) + \sigma_{inc} S_s(\alpha,\beta)\right) \quad (5)$$

where, σ_{coh} and σ_{inc} are the bound coherent and incoherent nuclear cross sections of the isotope, and T is the temperature of the material.

The current ENDF/B-VIII.0 ZrH_x TSLs were generated in the incoherent approximation within the LEAPR module of NJOY using the vibrational spectra calculated with the central force model developed at General Atomics (GA) [8–10], which is based upon the ϵ phase (i.e., ZrH_2). Nevertheless, these TSLs have historically been used to represent both phases in reactor physics calculations. Elastic scattering was assumed to be incoherent for both hydrogen and zirconium, such that $S_d^0 = 0$; an approximation which is reasonable for hydrogen due to its large incoherent nuclear scattering cross section. This approximation, however, neglects the effects of crystal structure important for scattering from zirconium bound in ZrH_x.

In this work the TSLs for hydrogen and zirconium bound in ZrH_x are generated from phonon spectra derived from *ab initio* lattice dynamics (AILD) and *ab initio* molecular dynamics (AIMD) for both δ-ZrH_x and ϵ-ZrH_2, thereby expanding the set of available sub-libraries for this material. These TSLs were generated using the Full Law Analysis Scattering System Hub (FLASSH), which includes a generalized coherent elastic scattering routine [11]. At this stage coherent elastic scattering only incorporates zirconium, enabling the sub-libraries to be extensible, within the limitations of the ENDF format, to the entire stoichiometry domain of each phase and mixed phase.

2. COMPUTATIONAL METHODS

The δ and ϵ phases of ZrH_x are characterized by cubic and tetragonal crystal structures, respectively [12]. For the purposes of *ab initio* calculations, the stoichiometry are represented as idealized $x = 1.5$ for δ phase and $x = 2$ for ϵ phase with unit cells shown in Figure 1. Initially the geometry of these structures were optimized through electronic structure calculations using VASP [13,14] with plane-augmented wave (PAW) pseudopotentials and a GGA-PBE exchange correlation functional [15,16]. A plane wave cutoff of 450 eV and k-mesh of less than 1.8 nm^{-1} were used and found to be sufficient for energy convergence of less than 4 meV/atom. The predicted lattice parameter of the δ phase are $a = 0.477$ nm, which is in good agreement with the experimental value of $a = 0.478$ nm [12]. The predicted ϵ phase parameters of $a = 0.354$ nm and $c = 0.440$ nm are also in reasonable agreement with experiment, $a = 0.352$ nm and $c = 0.445$ nm [12].

The phonon density of states (DOS), which is the fundamental input to the generation of TSL in the incoherent approximation, was generated in the harmonic approximation for δ-$ZrH_{1.5}$ and ϵ-ZrH_2 using AILD methods involving the coupling of the VASP [13,14] and PHONON [17] codes, described in Ref. [18]. Hellman-Feynman forces were extracted from VASP cacluations of $2 \times 2 \times 2$ (80 atoms) δ-$ZrH_{1.5}$ and $2 \times 2 \times 3$ (72 atoms) ϵ-ZrH_2 supercells with the previously listed convergence parameters. The forces describing the small displacements of zirconium atoms are expected to be well characterized within the harmonic approximation; however, hydrogen –due to its small mass and large vibrational displacement– may have significant anharmonic contributions to its

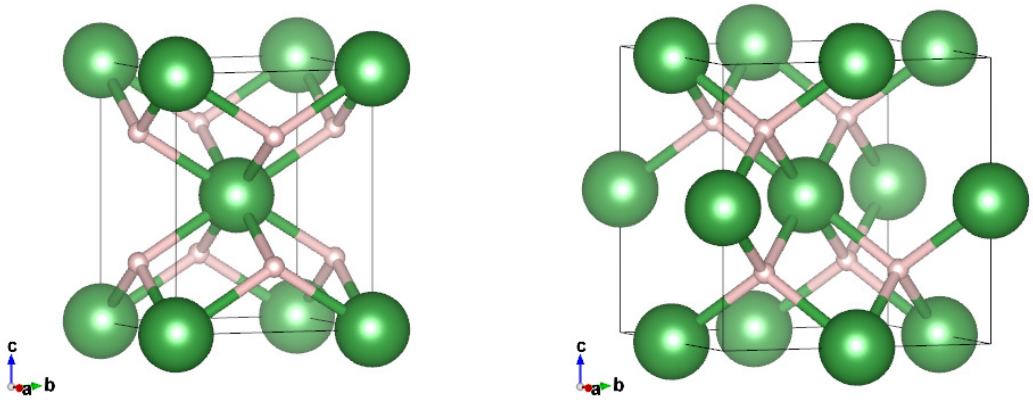

Figure 1: Crystal unit cell for ϵ-ZrH_2 (left) and δ-$ZrH_{1.5}$ (right).

motion even at 0 K (i.e., zero-point motion). AIMD simulations, which inherently include anharmonicity, were therefore performed using methods developed in previous work [19] to generate the hydrogen DOS. Using a reduced 350 eV planewave cutoff and a $1 \times 1 \times 1$ k-mesh, a $3 \times 3 \times 3$ (270 atoms) δ-$ZrH_{1.5}$ and $4 \times 4 \times 3$ (288 atoms) ϵ-ZrH_2 supercell were first allowed to equilibrate for 1 ps at 0.00025 ps timesteps using a 300 K NVT thermostat. Atomic trajectories were then evolved for an additional 1.5 ps. Subsequently, the velocities at each timestep were used to generate the phonon DOS for hydrogen as the Fourier transform of velocity auto-correlation function, which at 300 K captures intrinsic anharmonic effects without introducing significant spectral broadening.

The resulting hydrogen phonon DOS from AIMD, as seen in Figure 2, are shifted to lower energies compared to AILD calculations and are more consistent with inelastic neutron spectroscopy (INS) measurements. Additionally, the AIMD DOS are more analogous to experiment than the GA spectrum used in the current ENDF evalution [8,10], that has been previously noted to be qualitatively different from the experimental spectra [5,20]. Although the difference between the approximate AILD and AIMD average phonon energies is less than 0.01 eV, the deviation has an increasingly large impact on the predicted TSL and corresponding cross section for neutron scattering events with hydrogen involving the emission of multiple phonons. Specifically, the predicted oscillations using an AILD spectra diverge from experimental observation. Consequently, the AIMD phonons for hydrogen are expected to be more suitable for use in the generation of TSL.

TSL for zirconium and hydrogen in δ-ZrH_x (Zr(ZrH_x) and H(ZrH_x)) as well as zirconium and hydrogen in ϵ-ZrH_2 (Zr(ZrH_2) and H(ZrH_2)) were generated in the incoherent approximation as File 7 (MF=7) thermal scattering sub-libraries (NSUB=12) in ENDF-6 format [21] using the FLASSH code [11]. Each File 7 included evaluation of the TSL for temperatures between 296 K and 1200 K. The bound and free nuclear scattering cross sections (1 b = 10^{-28} m^2) used for each element are listed in Table 1 and were derived from relevant data in the NIST neutron scattering length database and ENDF/B-VIII.0 neutron reaction sub-libraries (at $E = 0.0253$ eV from File 3 MT=2 processed

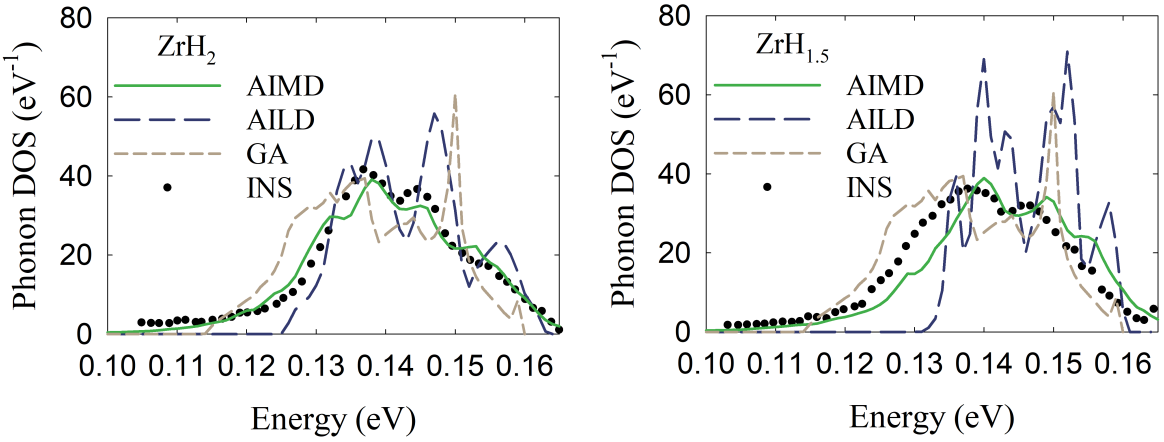

Figure 2: Phonon DOS for hydrogen in ZrH_2 (left) and $ZrH_{1.5}$ (right) compared to INS [5].

at 0 K) [22,23]. The zirconium File 7 corresponds to the natural isotopic mixture as reported in IUPAC atomic weight and isotopic abundance evaluations [24,25]. The phonon DOS used for zirconium and hydrogen were from AILD and AIMD simulations, respectively. A phonon order of 300 was used in the phonon expansion of all inelastic reactions (MT=4).

Table 1: Elemental Scattering Cross Sections

Element	A	σ_{coh} (b)	σ_{inc} (b)	σ_{free} (b)
Zr	90.4399	6.633485	—	6.780990
H	0.999167	1.7583	80.05416	20.43608

The coherent elastic scattering due to crystalline structure of each phase was computed using the generalized elastic scattering routine in FLASSH and stored on the corresponding elastic reaction (MT=2) of the zirconium File 7. The Debye-Waller matrix in the present work was computed in the cubic approximation. Although hydrogen has an appreciable coherent scattering length (-3.7 fm) when compared to zirconium (7.3 fm) [22,23], the contribution of the hydrogen sublattice was neglected so that the TSL is extensible across the entire stoichiometric range of each phase.

The hydrogen TSLs used the incoherent nuclear scattering option for MT=2. The nuclear scattering cross section stored on this reaction is only the nuclear incoherent scattering cross section (i.e., assumes $S_d^0 + S_s^0 = 0$), whereas the total free atom cross section is used for MT=4, per Eq. 5. This treatment, while in contrast to the current ENDF/B-VIII.0 which uses the total cross section for MT=2, is both consistent with the neglection of the hydrogen contribution to coherent elastic scattering and the treatment of nitrogen in uranium mononitride, which like hydrogen has non-negligible coherent and incoherent nuclear scattering cross section.

3. THERMAL SCATTERING LAWS

Inelastic neutron scattering techniques provide the direct measure of the double differential cross section of a compound, and via Eq. 5 are also directly calculable from the TSL. The double differential scattering cross section for ZrH_2 generated in the present work at the Naval Nuclear Laboratory (NNL) is compared to experiment and ENDF/B-VIII.0 in Figure 3. The anticipated oscillatory behavior due to the localized higher energy hydrogen phonon DOS is observed, whereby peaks occur at intervals of approximately 0.14 eV of energy loss. Both the Naval Nuclear Laboratory and current ENDF TSL demonstrate reasonable agreement with experiment [26]. Despite the similar calculated TSLs, a slight divergence occurs in each subsequently increasing energy loss peak due to differences in the average hydrogen phonon energy; however, as noted previously, the Naval Nuclear Laboratory phonon DOS more closely resembles experiment.

The differential scattering cross section of $ZrH_{1.92}$, shown in Figure 3, is computed as an integral of Eq. 5 over all scattered neutron energies. The Naval Nuclear Laboratory TSL and ENDF TSL provide similar predictions and trend well with experiment [27]. These calculations exclude the contribution of coherent elastic scattering from the Naval Nuclear Laboratory cross section, so the powder diffraction pattern predicted from the coherent elastic reaction of the zirconium Naval Nuclear Laboratory TSL is also shown. Deviation from experiment in the calculated differential cross sections at low scattering cosine are due to the use of the incoherent nuclear scattering cross section as opposed to the total elastic reaction, MT=2, of Naval Nuclear Laboratory TSLs. At low incident neutron energies where coherent elastic scattering is significant, diffraction peaks occur in the experimental data that result in a deviation from the continuous differential behavior of the calculations. Overall the calculated diffraction pattern matches these peaks, thereby demonstrating the importance of this contribution for the prediction of angular distributions.

The inelastic contributions to the Naval Nuclear Laboratory TSLs for both δ-ZrH_x (H(ZrH_x), Zr(ZrH_x)) and ϵ-ZrH_2 (H(ZrH_2), Zr(ZrH_2)) are illustrated in Figure 3 at temperatures of 296 K and 700 K, where the latter represents the estimated maximum fuel temperature of a 2 000 MW pulse in a TRIGA reactor [3]. In general the TSLs for hydrogen and zirconium are similar between the two phases. The zirconium TSLs indicate a quasi-elastic scattering spectrum at low momentum transfers, trending toward a free gas behavior at large momentum transfer (e.g., $\alpha = 1.979$). Oscillation in the hydrogen TSLs strongly favors energy loss ($\beta < 0$) at 296 K, but has a significant contribution from 0.14 eV 1-phonon upscattering events at 700 K. This behavior is a contributor to the strong negative moderator feedback coefficient in TRIGA systems. At low momentum transfers (e.g., $\alpha = 0.4943$) 1-phonon events are dominant; however, as the momentum transfer increases the possibility of downscattering involving multiple phonons becomes likely, exemplified by $\alpha = 5.067$. Although, the multi-phonon peaks occuring at integer values of approximately 0.14 eV are similar for the two phases, oscillations diverge with increasing $|\beta|$ due the a small increase in the average phonon energy of δ relative to the ϵ phase, that is also observed in experiment [5].

Integrated total scattering cross sections for δ-ZrH_x and ϵ-ZrH_2 were generated using NDEX nuclear data processing package and are shown in Figure 4. NDEX uses the the β grid tabulated on the TSL and an adaptive energy mesh to provide high resolution cross sections [28] which, as demonstrated in previous work [29], is important for metal hydride moderators where the coarse fixed energy meshes used in other codes (e.g., NJOY [9]) may lose the oscillatory behavior. Several

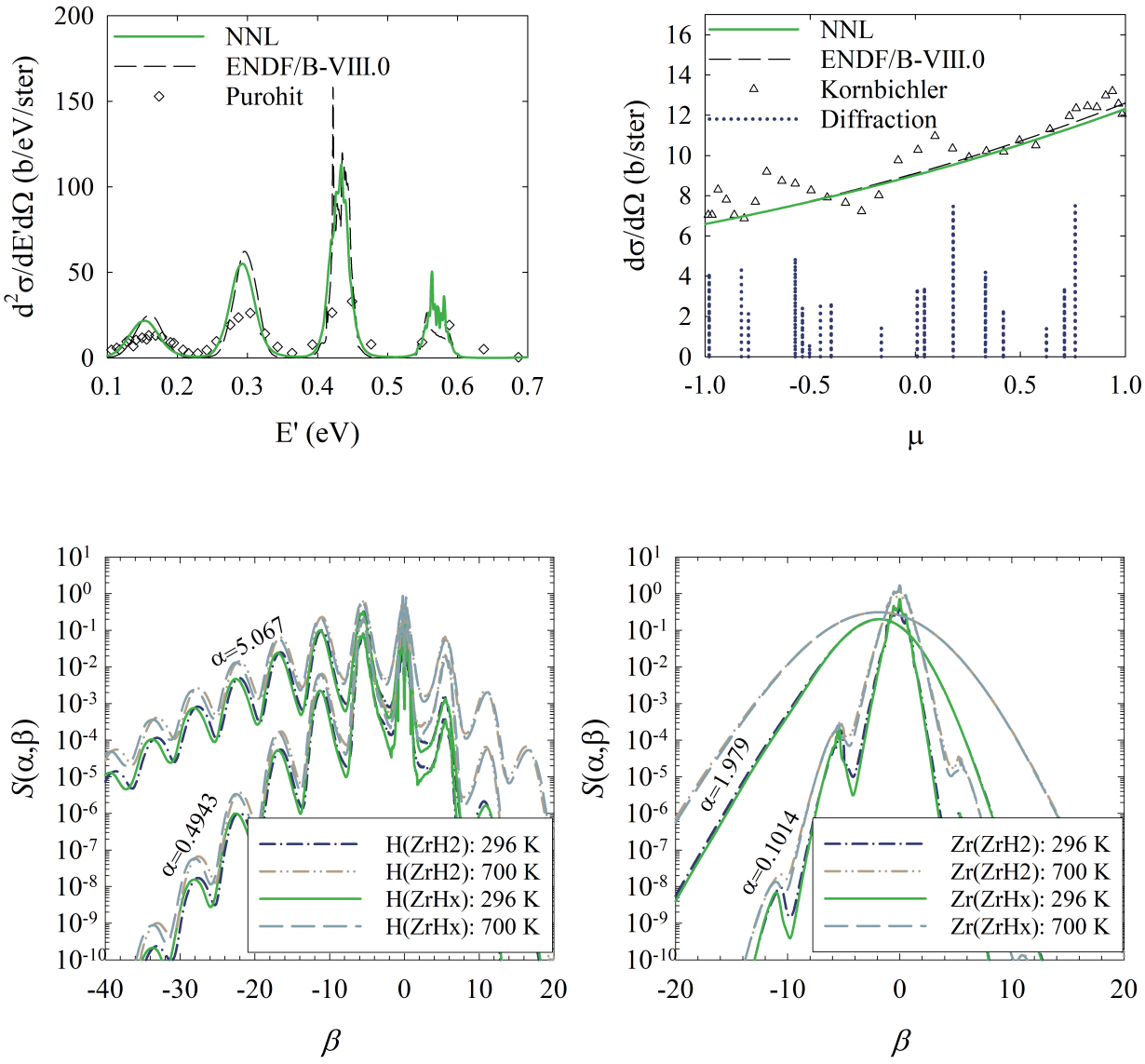

Figure 3: Double differential cross section of ZrH_2 for E=0.572 eV and μ=0.766 (top left) and differential cross section of ZrH_2 for E=0.0225 eV (top right) compared to experiment, Purohit [26] and Korbichler [27]. TSL for H (bottom left) and Zr (bottom right) in δ-ZrH_x and ϵ-ZrH_2 at 296 K and 700 K. Both α and β are referenced to 293.6 K.

compositions were selected for comparason between the two models and experiment, with $x = 1.6$ for δ phase and $x = 2$ for ϵ phase representing TRIGA and SNAP-10A fuel, respectively [1,3]. Each cross section is illustrated at room and elevated temperatures, with 700 K corresponding to pulse characteristics of a TRIGA and 800 K corresponding to the approximate max operating temperature of SNAP-10A [1].

At 296 K, the impact of changes in the coherent and incoherent elastic scattering is appreciable for both phases, resulting in a 6-10 b difference in the total scattering cross section below the Bragg edge between the Naval Nuclear Laboratory and current ENDF evaluations. In particular the Bragg peak at 0.0027 and 0.0036 eV in the δ-ZrH Naval Nuclear Laboratory evaluation is in reasonable agreement with experimental data [3], but are absent from the current ENDF evalution. Below the Bragg cut-off (0.0027 eV) the elastic behavior is between Naval Nuclear Laboratory and ENDF, consistent with the neglect of coherent elastic effects of hydrogen (e.g., correlated hydrogen vacant sites). Additionally, $ZrH_{1.6}$ shows a parallel $1/v$ trend between the Naval Nuclear Laboratory and ENDF evaluations in this region, whereas ZrH_2 diverges with a less pronounced $1/v$ behavior in the Naval Nuclear Laboratory evaluation. This disparity arises from a decreased contribution of low energy (< 0.03 eV) phonons in the ϵ phase compared to the δ phase, present in both AILD and AIMD calculations.

As temperature increases, inelastic scattering with hydrogen begins to dominate and 0.14 eV 1-phonon upscatter becomes the primary contributor to the $1/v$ scattering cross section. Consequently, the total scattering cross sections for the Naval Nuclear Laboratory and ENDF evaluations are nearly the same at 700 K and 800 K; however, an observable consequences of coherent elastic scattering on the total scattering cross section persist between approximately 0.001-0.004 eV. At incident energies above 0.05 eV, both calculated cross sections trend well with experiment. In this range inelastic scattering causes oscillations in the cross section at intervals of approximately 0.14 eV that broaden with increasing temperature, and quantitative differences between Naval Nuclear Laboratory and ENDF evaluations arising primarily from a 0.4 b difference in the free atom cross section used in the generation of the zirconium TSLs.

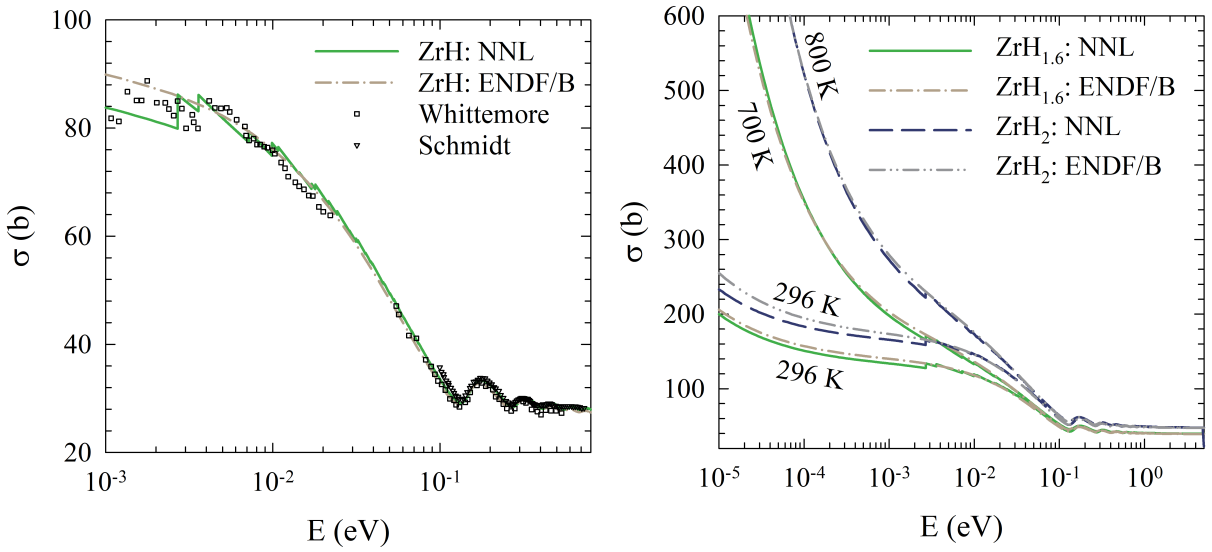

Figure 4: Scattering cross section of δ-ZrH compared to experiments at room temperature, Whittemore [6] and Schmidt [30] (left). Scattering cross sections of δ-$ZrH_{1.6}$ and ϵ-ZrH_2 compared to current ENDF/B-VIII.0 evaluations (right).

4. CONCLUSIONS

Phonon spectra for hydrogen and zirconium in δ and ϵ zirconium hydride were developed using predictive AIMD and AILD simulations. Subsequently, these spectra were used in the FLASSH code to generate new TSL evaluations for zirconium hydride which include, for the first time, the previously neglected contribution of coherent elastic scattering in multiple phases of this material. These evaluations include both δ-ZrH_x (H(ZrH_x) and Zr(ZrH_x)) and ϵ-ZrH_2 (H(ZrH_2) and Zr(ZrH_2)) permitting explicit modeling of each phase in reactor physics calculations or benchmarks (e.g., TRIGA, SNAP-10A) across the entire range of their stoichiometry. Currently only a single sub-library set (H(ZrH) and Zr(ZrH)) is included in the ENDF evaluation for this material, such that the new Naval Nuclear Laboratory evaluations may be considered not only a re-evaluation but also an expansion of the ENDF/B library database. Moreover, differences in both the coherent elastic reaction and hydrogen phonon spectra provide evidence that separate treatment of the δ and ϵ phases in neutronics calculations may be important for some applications.

REFERENCES

[1] A. F. Lillie, D. T. McClelland, W. J. Roberts and J. H. Walter, "Zirconium Hydride Fuel Element Performance Characteristics," AI-AEC-13084, Atomics International Division (1973).

[2] E. Zuzek, J. P. Abriata, A. San-Martin and F.D. Manchester, "The H-Zr (Hydrogen-Zirconium) System," *Bulletin of Alloy Phase Diagrams*, **11**, pp. 385-395 (1990).

[3] "Kinetic Behavior of TRIGA Reactors," GA-7882, General Atomics (1967).

[4] J. Bair, M. A. Zaeem and M. Tonks, "A review of hydride precipitation in zirconium alloys," *J. Nucl. Mater.*, **446**, pp. 12-20 (2015).

[5] J. G. Couch, O. K. Harling and L. C. Clune, "Structure in the neutron scattering spectra of zirconium hydride," *Phys. Rev. B*, **4**, pp. 2675-2681 (1971).

[6] W. L. Whittemore, "Neutron Interactions in Zirconium Hydride," GA-4490, General Atomics (1964).

[7] A. I. Hawari, "Modern techniques for inelastic thermal neutron scattering analysis," *Nuclear Data Sheets*, **118**, pp. 172-175 (2014).

[8] R. E. MacFarlane, "New Thermal Neutron Scattering Files for ENDF/B-VI Release 2," LA-12639-MS, Los Alamos National Lab (1994).

[9] A. C. Kahler and R. E. MarFarlane, "The NJOY Nuclear Data Processing System, Version 2012," LA-UR-12-27079, Los Alamos National Lab (2012).

[10] E. L. Slaggie, "Central force lattice dynamical model for zirconium hydride," *J. Phys. Chem. Solids*, **29**, pp. 923-934 (1968).

[11] Y. Zhu and A. I. Hawari, "Full Law Analysis Scattering System Hub (FLASSH)," *Proceedings of PHYSOR 2018*, Canún, Mexico, April 22-26 (2018).

[12] C. P. Kempter, R. O. Elliot and K. A. Gschneider Jr., "Thermal expansion of delta and epsilon zirconium hydrides," *J. Chem. Phys.*, **33**, pp. 837-840 (1960).

[13] G. Kresse and J. Furthmüller, "Efficiency of ab initio total energy calculations for metals and semiconductors using a plane-wave basis set," *Comput. Mat. Sci.*, **6**, pp. 15-50 (1996).

[14] G. Kresse and J. Furthmüller, "Efficient iterative schemes for ab initio total energy calculations using a plane-wave basis set," *Phys. Rev. B*, **54**, pp. 11169-11186 (1996).

[15] P. E. Blöchl, "Projector augmented-wave method," *Phys. Rev. B*, **50**, pp. 17953-17979 (1994).

[16] J. P. Perdew, K. Burke and M. Ernzerhof, "Generalized gradient approximation made simple," *Phys. Rev. Lett.*, **77**, pp. 3865-3868 (1996).

[17] K. Parlinski, Z. Q. Li and Y. Kawazoe, "First-principles determination of the soft mode in cubic ZrO_2," *Phys. Rev. Lett.*, **78**, pp. 4063-4066 (1997).

[18] A. I. Hawari, I. I Al-Qasir, V. H. Gillette and B. W. Wehring, "Ab initio generation of thermal neutron scattering cross sections," *Proceedings of PHYSOR 2004*, Chicago, Illinois, April 25-29 (2004).

[19] J. L. Wormald and A. I. Hawari, "Generation of phonon density of states and thermal scattering law using ab initio molecular dynamics," *Prog. Nucl. Energy*, **101**, pp. 461-467 (2017).

[20] S. S. Malik, D. C. Rorer and G. Brunhart, "Optical-phonon structure and precision neutron total cross section measurements of zirconium hydride," *J. Phys. F: Met Phys.*, **14**, pp. 73-81 (1984).

[21] M. Herman and A. Trkov, "Data Formats and Procedures for the Evaluated Nuclear Data File ENDF/B-VI and ENDF/B-VII," BNL-90365-2009, Brookhaven National Laboratory (2009).

[22] V. F. Sears, "Neutron scattering lengths and cross sections," *Neutron News*, **29**, pp. 26-37 (1992).

[23] D. A. Brown et al., "ENDF/B-VIII.0: The 8^{th} major release of the nuclear reaction data library with CIELO-project cross sections, new standards and thermal scattering data," *Nuclear Data Sheets*, **148**, pp. 1-142 (2018).

[24] J. S. Coursey, D. J. Schwab, J. J. Tsai and R. A. Dragoset, "Atomic Weights and Isotopic Compositions (version 4.1)," National Institute of Standards and Technology, http://physics.nist.gov/Comp (2015).

[25] M. Berglund and M. E. Wieser, "Isotopic compositions of the elements 2009 (IUPAC Technical Report)," *Pure Appl. Chem*, **83**, pp. 397-410 (2011).

[26] S. N. Purohit et al., "Inelastic neutron scattering in metal hydrides, UC and UO2, and applications of the scattering law," *Neutron Thermalization and Reactor Spectra*, Vol. I, Ann Arbor, Michigan, July 17-21, pp 407-433 (1967).

[27] K. Parlinski, Z. Q. Li and Y. Kawazoe, "Bestimmung der diffusionskonstanten $D(E_0,T)$ und $<D_v(T)>$ thermischer neutronen in H_2O, Phenylen, $ZrH_{1.92}$ und D_2O durch messung der streuwinkelverteilungen. II. Zirkonhydrid und schweres wasser," *Nukleonik*, **78**, pp. 281 (1965).

[28] T. H. Trumbull, "Computational methods used to process thermal neutron scattering data for use in continous energy Monte Carlo codes," *Proceedings of PHYSOR 2016*, Sun Valley, Idaho, May 1-5 (2016).

[29] M. Zerkle and J. Holmes, "A thermal neutron scattering law for yttrium hydride," *EPJ Web of Conferences*, **146**, pp. 13005-13008 (2017).

[30] U. Schmidt, "Untersuchung der wasserstoff- und deuteriumschwingungen in metallhydriden, -hydrodeuteriden und -deuteriden mittles totaler neutronen- wirkunsquerschnitte" *ATKE*, **12**, pp. 385 (1967).